Biochemical Pharmacology, Vol. 45, No. 10, pp. 2063–2069, 1993.
Printed in Great Britain.

0006-2952/93 $6.00 + 0.00
© 1993. Pergamon Press Ltd

A MATHEMATICAL MODEL OF THE KINETICS AND TISSUE DISTRIBUTION OF 2-FLUORO-β-ALANINE, THE MAJOR CATABOLITE OF 5-FLUOROURACIL

RUIWEN ZHANG,* TIEPU LIU,† SENG-JAW SOONG† and ROBERT B. DIASIO*‡

*Department of Pharmacology and †Division of Biostatistics, Comprehensive Cancer Center, University of Alabama at Birmingham, Birmingham, AL 35294, U.S.A.

(*Received* 9 *October* 1992; *accepted* 19 *January* 1993)

Abstract—2-Fluoro-β-alanine (FBAL) is the major metabolite of 5-fluorouracil (FUra), one of the most widely used anticancer drugs. It has been suggested previously that FBAL and/or its metabolites may have a role in the hepatotoxicity, neurotoxicity and cardiotoxicity resulting from FUra chemotherapy. Studies in patients and experimental animals have demonstrated that FBAL has a prolonged elimination compared with the parent drug, FUra. In the present manuscript, a mathematical model is developed for the kinetics and tissue distribution of FBAL. This model is based on recently published data from a study of the pharmacokinetics and disposition of FBAL in rats (Zhang *et al.*, *Drug Metab Dispos* **20**: 113–119, 1992). Satisfactory agreement was achieved between predicted and measured values, permitting an accurate evaluation of the kinetic and distribution parameters for FBAL. This model indicates that: (1) FBAL accumulates in several tissues including brain, heart, spleen, and enterohepatic system; and (2) enterohepatic circulation of FBAL and its bile acid conjugates has an important role in FBAL kinetics and distribution as demonstrated by a model in which enterohepatic circulation parameters were deleted.

2-Fluoro-β-alanine (FBAL§) is the major catabolite of 5-fluorouracil (FUra) (Fig. 1), one of the most widely used anticancer drugs [1–3]. It has been suggested that FBAL and/or its metabolites may have a role in the neurotoxicity, cardiotoxicity, and hepatobiliary toxicity resulting from administration of FUra [4–10]. Studies from our laboratory [11–15] and others [16, 17] have demonstrated that FBAL is conjugated with bile acids (BA). These conjugates (FBAL–BA) are the major biliary metabolites after administration of FUra in both experimental animals and patients. It has also been demonstrated that FBAL–BA conjugates undergo extensive enterohepatic circulation (EHC) in rats, characterized by extensive deconjugation in the small intestine with reconjugation in the liver [18]. Based on these observations, a model of the EHC, metabolism and disposition of FBAL–BA conjugates in rats has been proposed [18].

Clinical pharmacokinetic studies from our laboratory have shown that FBAL has a prolonged elimination, with an approximately 150-fold longer half-life than its parent drug (FUra) in patients receiving FUra by i.v. bolus [19, 20]. The mechanism responsible for the delayed elimination of FBAL is not fully understood. Recently, we reported a comprehensive study of the kinetics and tissue distribution of FBAL in rats [21], which demonstrated that FBAL accumulated and was retained in specific tissues, suggesting that the pattern of accumulation and tissue distribution of FBAL may be related to the sites of FUra toxicity.

The data from the above study [21] were used to develop a mathematical model to describe the kinetics and tissue distribution of FBAL in rats following i.v. bolus administration of FBAL. The present manuscript reports the general assumptions of the model, the statistical methods used, and the estimated parameters for distribution and elimination of FBAL.

MATERIALS AND METHODS

Experimental data

The experimental design, materials, and methods used in the study of the kinetics and tissue distribution of FBAL were reported previously [21]. Since FBAL formed *in vivo* is the 2*R*-stereoisomer which is not commercially available, [^{3}H]FBAL used in the study was purified from either the urine of cancer patients receiving [6-^{3}H]FUra as part of an institution-approved protocol or the urine of rats to which [6-^{3}H]FUra had been administered [21]. Male Sprague–Dawley rats were utilized in the present study. Briefly, [^{3}H]FBAL was administered by i.v. bolus at 25 μmol/kg (5 μCi/kg) into the caudal vein of rats. Samples of blood, bile, urine, and feces were collected at various times from 0 to 192 hr. For the tissue distribution study, rats were killed at various times from 15 min to 192 hr. Tissue samples included liver, brain, eyes, lungs, heart, spleen, stomach, small and large intestines, kidneys, skeletal muscle, and fatty tissue.

The total FBAL-derived radioactivity in various tissues and body fluids was quantitated by liquid

‡ Corresponding author: Dr. Robert B. Diasio, Box 600 Volker Hall, Department of Pharmacology, University of Alabama at Birmingham, Birmingham, AL 35294-0019. Tel. (205) 934-4578; FAX (205) 934-8240.

§ Abbreviations: FBAL, 2-fluoro-β-alanine; FUra, 5-fluorouracil; BA, bile acids; EHC, enterohepatic circulation; WLS, weighted least squares; and AIC, Akaike Information Criterion.

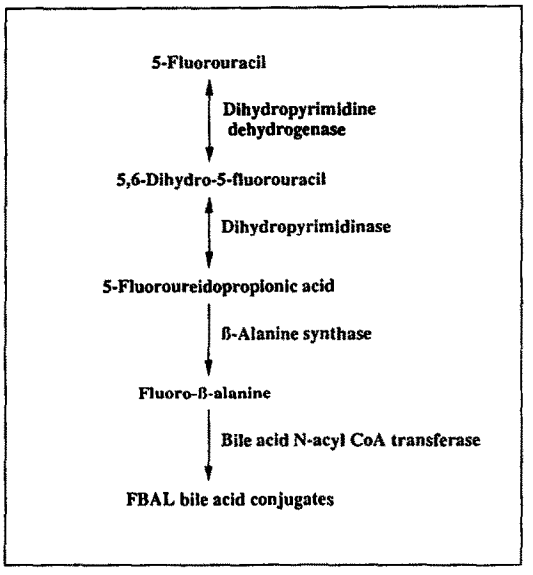

Fig. 1. Catabolism of 5-fluorouracil in humans and experimental animals.

scintillation spectrometry; the chemical forms oriented with the radioactivity in these samples were determined by reversed-phase HPLC analysis [21]. The concentrations of FBAL and/or its metabolites were expressed as FBAL equivalents in either nanomoles per milliliter of body fluids or nanomoles per gram of tissue (or feces).

Modelling

General assumptions. The model was based on data from the above study [21]. Following i.v. bolus administration, FBAL was distributed into various tissues and body fluids. The concentrations of FBAL-derived radioactivity were obtained at various times over 192 hr. Preliminary analysis suggested that a linear compartmental model fits the plasma, bile and urine data adequately [21]. Therefore, we assumed that the distribution of FBAL in each tissue follows linear first-order kinetics.

Mathematical formulation. To develop a mathematical model, we assumed that the process of FBAL distribution in the body could be described by a set of differential equations—state equations [22–24]. For a set of linear first-order differential equations, the general form is:

$$\frac{dX_i}{dt} = \sum_{j=1}^{n} k_{j-i} X_j - \sum_{j=0}^{n} k_{i-j} X_i, X_i(0) = c \quad \text{for } i = 1, \ldots, n$$

where X_i is the state variable representing the concentration of FBAL in each compartment (tissue or body fluids), and k_{i-j} is the rate constant from compartment i to compartment j. When $j = 0$, k_{i-j} (k_{i-o}) is the rate constant from compartment i to the environment. If there is no transfer from compartment i to compartment j, the rate constant k_{i-j} is equal to 0. $X_i(0)$ is the initial concentration of FBAL in each compartment, which is 0 for every tissue or body fluid except plasma. The initial plasma concentration is assumed to be proportional to the i.v. bolus dose of FBAL administered into rats.

Statistical methods. The vector of parameters θ to be estimated in the model was the rate constant (k_{i-j}). The weighted least squares (WLS) method was used for estimation of these parameters. The WLS objective function is:

$$O_{WLS} = \sum_{i=1}^{p} \sum_{j=1}^{m_i} W_{ij}(z_i(t_j) - y_i(\theta, t_j))^2$$

where $z_i(t_j)$ is the measured concentration of tissue (or body fluid) i at time j, $y_i(\theta, t_j)$ is the predicted concentration from the model, p is the number of compartments (tissues or body fluids) in the model, and m_i is the number of measurements in the ith compartment. The weight W_{ij} was the product of the weight for each model output (g_i, $i = 1, \ldots, p$) and the weight for each of the measurements (w'_{ij}, $j = 1, \ldots, m_i$). During the initial modelling, g_i was set equal to the mean concentration of each of the tissues or body fluids or 1. The setting, $g_i = 1$, was used in the final model. w'_{ij} was set equal to the inverse of the variance of the measurement ($w'_{ij} = 1/\sigma^2_{ij}$). σ_{ij} was set as a linear function of the measurement ($\sigma_{ij} = a_i z_i(t_j) + b_i$). The minimum and maximum concentration measurements of each tissue and their standard deviation assumed as 10–15% of the measurements were used to define a_i and b_i.

To minimize the WLS objective function and obtain the least squares estimates, the Nelder–Mead simplex algorithm was used [25]. The standard error of each parameter estimate was obtained from the asymptotic covariance matrix of the estimated parameters which was used to calculate the 95% confidence interval for each estimated parameter.

Assuming that the measurement error of each data point, $z_i(t_j)$, was generated from a Gaussian distribution with a zero mean and a variance proportional to σ^2_{ij}, the weighted least squares estimators are equivalent to those from maximum likelihood estimation. This permitted use of the Akaike Information Criterion (AIC) to select the best model. The criterion is defined as AIC = O_{WLS} + $2n_\theta$, which gives a measure of the goodness of fit of the model with consideration of the number of parameters (n_θ) in the model. The model with the smallest AIC was chosen [26].

Computational methods. A Fortran program, ADAPT II, was used for estimation of the model parameters [25]. Computations were performed on a DEC VAX 6210 computer. The ADAPT II program uses the differential equation solver LSODA (Livermore Solver for Ordinary Differential equations with Automatic method switching for stiff and nonstiff problems), which uses variable order, variable step size formulations of Adam's method and Gear's method as the nonstiff and stiff equation solvers, respectively.

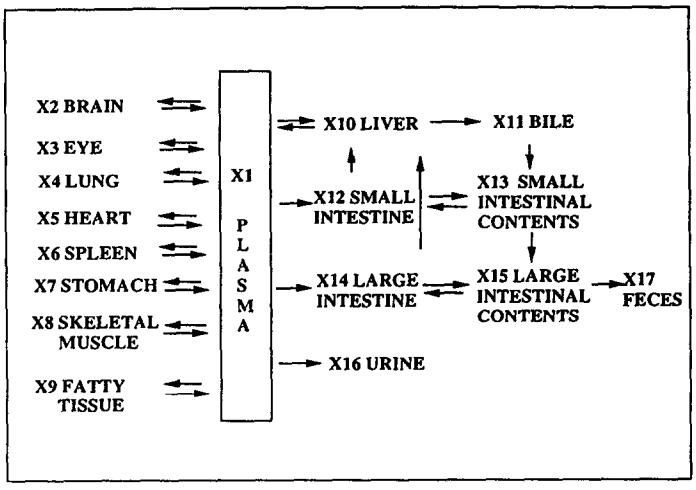

Fig. 2. Preliminary model with all tissues and body fluids.

RESULTS

Selection of compartments and working model

Since we had the time–concentration data for 17 tissues (or body fluids), we initially utilized a working model that included all tissues or body fluids, as shown in Fig. 2. As expected, the model fit some of the tissues unsatisfactorily, and also made estimation of parameters and their variances very difficult because of limited data points. We subsequently developed two separate models: one model including the enterohepatic system, and another including all the other tissues and body fluids without the enterohepatic system.

In developing the present model, our main purpose was to predict the effect and importance of each compartment in the distribution process of FBAL. We attempted to follow the disappearance of FBAL from plasma and set the plasma concentration of FBAL as a linear function of the concentration of each of the other compartments. At the $\alpha = 0.05$ level, X_{10} (liver) was selected by stepwise regression analysis with an $R^2 = 78.8\%$. At both the $\alpha = 0.15$ and $\alpha = 0.25$ levels, with the same group of compartments, X_2 (brain), X_6 (spleen), X_{11} (bile), X_{12} (small intestine), X_{13} (small intestinal contents) and X_{16} (urine) were selected in the model, with an $R^2 = 87.9\%$. Stepwise regression analysis permitted selection of the most important tissues (or body fluids) that are significantly correlated with the plasma concentrations.

Final model

Following the linear regression analysis and evaluation of the above two working models, we concluded that a model with 10 compartments provided the best fit to the data. The structure of

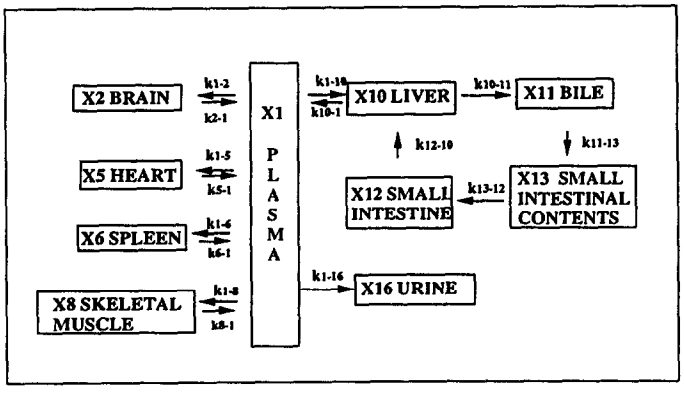

Fig. 3. Final model with 10 compartments (tissues or body fluids). k_{i-j} represents the rate constant for transfer of FBAL (and its metabolites) from compartment i to compartment j. All exchanges were modeled by first-order kinetics. Estimates of these rate constants are shown in Table 2. In the final model, 4 compartments represent the enterohepatic system, including liver (X_{10}), bile (X_{11}), small intestine (X_{12}), and small intestinal contents (X_{13}).

Table 1. Estimates of rate constants of FBAL distribution

k^*_{i-j}	Estimate	95% Confidence intervals	
k_{1-2}	0.02436	0.02308	0.02564
k_{2-1}	0.0008599	0.0007071	0.001013
k_{1-5}	0.02484	0.02351	0.02617
k_{5-1}	0.0007800	0.0006406	0.0009194
k_{1-6}	0.03196	0.02975	0.03418
k_{6-1}	0.0008965	0.0007187	0.001074
k_{1-8}	0.01373	0.01313	0.01432
k_{8-1}	0.0008624	0.0007169	0.001008
k_{1-10}	1.029	0.9657	1.0930
k_{10-1}	0.4690	0.4256	0.5124
k_{10-11}	0.02932	0.02694	0.03170
k_{11-13}	0.01744	0.01468	0.02021
k_{12-10}	0.001482	0.001208	0.001755
k_{13-12}	0.002622	0.002272	0.002973
k_{1-16}	0.01217	0.01001	0.01433

* k_{i-j} Values are the rate constants (per minute) for FBAL transfer from compartment i to compartment j, as depicted in Fig. 3.

this model is shown in Fig. 3, which gave the smallest AIC value of 45630.5. In the final model, 15 parameters (rate constants) were estimated as illustrated in Table 1 with 95% confidence intervals. Figure 4 shows the time–concentration distribution of FBAL in selected tissues and body fluids, including plasma, bile, and liver with actual measurements and predicted values from the model as well. These results indicate that satisfactory agreement was achieved between measured and predicted values, which enables an accurate evaluation of the kinetics and distribution of FBAL.

As illustrated in Table 1, FBAL influx rate constant in the brain (k_{1-2}) was greater than its efflux rate constant (k_{2-1}), indicating that an uphill uptake system may exist, resulting in accumulation of FBAL in the brain. A similar uphill uptake of FBAL was also predicted in the heart ($k_{1-5} \gg k_{5-1}$), spleen ($k_{1-6} \gg k_{6-1}$), skeletal muscle ($k_{1-8} \gg k_{8-1}$), and liver ($k_{1-10} > k_{10-1}$).

Differences in the rate constants for the transfer from plasma to the various compartments can be used to predict the importance of these compartments in the kinetics and/or elimination of FBAL. For example, FBAL influx rate constant in the liver (k_{1-10}) was much greater than other tissues (Table 1), suggesting that the liver (and enterohepatic system) has the most important role in controlling FBAL distribution and elimination.

Effect of EHC on FBAL distribution

To examine further the importance of EHC of FBAL (and its metabolites), we developed a modified model by deleting the EHC from the final model shown in Fig. 3. In this modified model, compartments representing the enterohepatic system, including liver (X_{10}), bile (X_{11}), small intestine (X_{12}), and small intestinal contents (X_{13}), were deleted, and the rate constants (k'_{i-j}) of the remaining compartments were estimated as illustrated in Table 2. Compared with the final model, deleting the EHC

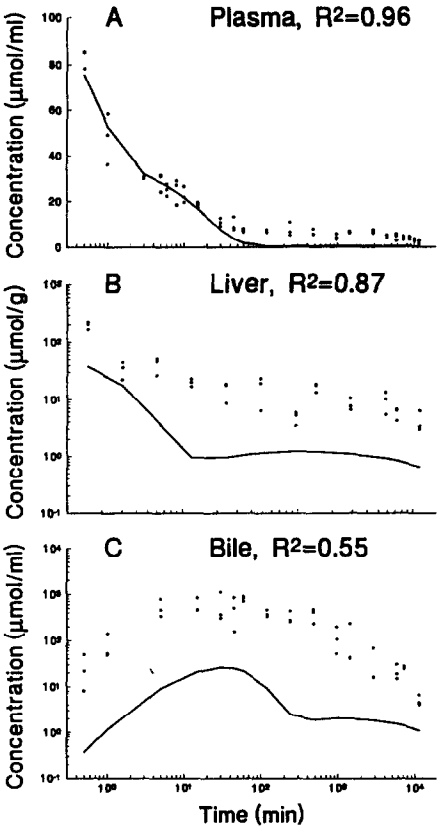

Fig. 4. Fitting the final model to the data of the study of FBAL kinetics and distribution following i.v. administration of radiolabeled FBAL in rats. *Dot symbols* represent the actual measurements; *solid lines* represent the time profiles predicted by the final model.

Table 2. Estimates of rate constants of FBAL distribution without EHC

k'_{i-j}*	Estimate	95% Confidence intervals	
k'_{1-2}	0.06769	0.06501	0.07037
k'_{2-1}	0.0001564	0.0001413	0.001715
k'_{1-5}	0.07523	0.07222	0.07823
k'_{5-1}	0.0002148	0.0001949	0.0002347
k'_{1-6}	0.09522	0.09057	0.09988
k'_{6-1}	0.0002495	0.0002151	0.0002838
k'_{1-8}	0.03284	0.03169	0.03398
k'_{8-1}	0.0001358	0.0001265	0.001452
k'_{1-16}	0.1832	0.1762	0.1902

* k'_{i-j} Values are the rate constants (per minute) for FBAL transfer from compartment i to compartment j in the modified model in which the EHC of FBAL (and its metabolites) was deleted (see text).

in the modified model resulted in an increase of influx rate constants and a decrease of efflux rate constants for several tissues, including brain ($k'_{1-2} > k_{1-2}$, $k'_{2-1} < k_{2-1}$), heart ($k'_{1-5} > k_{1-5}$, $k'_{5-1} < k_{5-1}$),

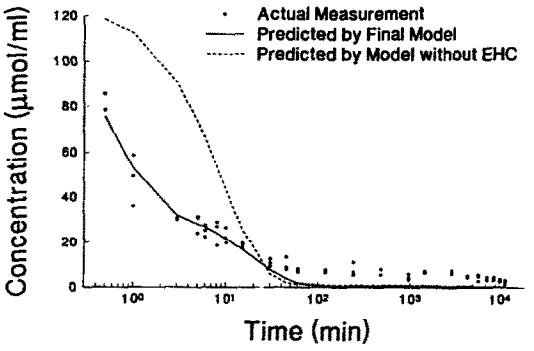

Fig. 5. Effect of EHC on FBAL plasma concentration. *Dot symbols* represent the actual measurements of FBAL plasma concentrations; *solid line* represents the time profile predicted by the final model shown in Fig. 3; and *dash line* represents the time profile predicted by the modified model in which the EHC and FBAL (and its metabolites) were deleted from the final model.

spleen ($k'_{1-6} > k_{1-6}$, $k'_{6-1} < k_{6-1}$) and skeletal muscle ($k'_{1-8} > k_{1-8}$, $k'_{8-1} < k_{8-1}$). These results further demonstrate that EHC has an important role in the distribution of FBAL. Without EHC, two events are predicted to occur: more FBAL will accumulate in those tissues outside the enterohepatic system and more will be eliminated through urine (since $k'_{1-16} \gg k_{1-16}$).

The importance of EHC on FBAL kinetics was demonstrated further by the difference of FBAL plasma disappearance predicted by the final model and the modified model as shown in Fig. 5. In the modified model, assuming the same rate constants (both influx and efflux) for all other tissues outside EHC as estimated in the original model, deleting EHC resulted in a significant change of FBAL plasma disappearance: higher plasma levels in the earlier phase (initial 10 min) and lower levels in the later stage were predicted, suggesting that, without EHC, more FBAL will accumulate in tissues in the earlier phase (because of high plasma concentration) and more FBAL will be eliminated through urine.

DISCUSSION

The present manuscript is the first report that describes the pharmacokinetics and distribution of FBAL, the major metabolite of FUra, by introducing a multi-compartmental mathematical model based on the published data from a comprehensive study in rats [21]. Preliminary analysis of the above data suggested that: (1) FBAL accumulates in several tissues that may be correlated with the sites of FUra toxicity; (2) correlation and regression analysis showed the relative importance of each tissue on FBAL kinetics and permitted selection of the compartments in developing a mathematical model; and (3) a linear compartmental model fits the plasma, bile, and urine FBAL data adequately and allowed us to assume that the distribution of FBAL in each compartment follows linear first-order kinetics. The final model with 10 compartments and 15 parameters best fits the actual measurements. The estimates of rate constants in the final model were significant at the $\alpha = 0.05$ level as reflected by their 95% confidence intervals which did not include 0 (Table 1).

Closer examination of the final model demonstrates that it predicts the significance of each compartment (tissue or body fluid) in FBAL kinetics and distribution not only qualitatively (Fig. 3) but also quantitatively (Tables 1 and 2, Fig. 5). This model predicts that an accumulation of FBAL (and its metabolites) will occur in the brain, heart, spleen, skeletal muscle, and the enterohepatic system (Table 1) by showing that the rate constant of influx for each compartment was significantly greater (by 2- to 36-fold) than that of efflux. The comparison of rate constants of influx (uptake from the plasma into each tissue) also predicts the relative importance of each tissue in the determination of FBAL distribution. As illustrated in Table 1, the influx rate constant for the liver was 40- to 70-fold greater than that for the brain, heart, spleen or skeletal muscle. Further analysis demonstrated that the high uptake of FBAL into the liver was due to the extensive EHC. Evidence for the importance of EHC on FBAL kinetics and distribution derives from the modified model in which the EHC of FBAL (and its metabolites) was deleted. Without EHC, more FBAL would accumulate in other tissues and/or more FBAL would be excreted through urine.

The accumulation of FBAL (and its metabolites) in several tissues was observed in our previous studies [18, 21]. The present mathematical model further predicted that FBAL will accumulate in the brain, heart, spleen, skeletal muscle, and enterohepatic system. Although the mechanism(s) responsible for the accumulation is unclear, an uphill transport system was predicted in this mathematical model.

The accumulation of FBAL in specific tissues deserves additional comment. Although FUra has been used in the clinic for more than 3 decades, the mechanisms responsible for its toxicities are not fully understood. The cytostatic effects of FUra are usually used to explain the toxicities in rapidly growing tissues such as bone marrow and gastrointestinal mucosa. However, neurotoxicity and cardiotoxicity cannot be easily explained by this mechanism. Since FBAL is the major metabolite of FUra and accumulates in brain and heart, it may have an important role in the neurotoxicity and cardiotoxicity observed with FUra. Studies in experimental animals [6–9] have shown that FBAL has direct toxicity on nervous tissue, which is similar to the pathologic changes resulting from administration of FUra. The present model predicted an uphill uptake system for FBAL in brain. FBAL has a chemical structure similar to that of β-alanine, an important neurotransmitter [27]. Uphill transport and accumulation of FBAL in nervous tissue may affect the metabolism of β-alanine and its biological function. Further studies are needed.

Similarly, accumulation of FBAL in the heart may also be important in the development of FUra cardiotoxicity. Considering that FBAL has a chemical

structure similar to taurine, which is known to have an important role in cardiovascular function [28], its uphill transport and accumulation in the heart may affect the uptake and function of taurine.

Since FBAL is conjugated with BA in the liver [10–16] and FBAL–BA conjugates undergo extensive enterohepatic circulation [18], it is of interest to investigate the significance of EHC of FBAL and its BA conjugates. The present model further demonstrated that the EHC of FBAL has an important role in the determination of FBAL kinetics and distribution. The EHC of FBAL and FBAL–BA conjugates includes conjugation (and reconjugation) in the liver, deconjugation in the small intestine, and absorption and transport of FBAL, BA, and FBAL–BA through the intestinal wall and hepatobiliary system. Since FBAL shares the same enzymatic mechanism in BA conjugation and deconjugation as the physiological amino acids, taurine and glycine, its metabolism and EHC may affect normal metabolism and function of amino acids and bile acids. Future studies are needed to evaluate the mechanism of transport of FBAL and its BA conjugates across the intestinal wall and hepatobiliary membrane.

In conclusion, a multicompartmental mathematical model of kinetics and tissue distribution of FBAL is proposed in the present manuscript based on the published data from a recent study in rats. This model predicts qualitatively and quantitatively an uphill transport and accumulation of FBAL in specific tissues, which may be related to the sites of FUra toxicities. The EHC of FBAL (and its BA conjugates) was shown to have an important role in determination of FBAL distribution. The model may be helpful in the future studies of FBAL toxicity as well as FUra pharmacology. However, we realize that there are limitations in this model, e.g. the model does not fit the data at low concentrations in the late stage very well (this may be due to limited data points), and differences between predicted and actual measurements still remain for some tissues (this may be due to the limited number of compartments chosen in the final model with others being omitted). Further studies are needed to improve the model, including collection of more data (especially in the late stage) and detailed investigations on biochemical processes such as transport of FBAL and its metabolites, conjugation and deconjugation of FBAL bile acid conjugates, and plasma flow rate in each compartment.

REFERENCES

1. Chabner BA and Myers CE, Clinical pharmacology of cancer chemotherapy. In: *Cancer: Principles and Practice of Oncology* (Eds. De Vita VT, Hellman S and Rosenberg SA), 3rd Edn, pp. 349–395. Lippincott, Philadelphia, 1989.
2. Diasio RB and Harris BE, Clinical pharmacology of 5-fluorouracil. *Clin Pharmacokinet* **16**: 215–237, 1989.
3. Daher GC, Harris BE and Diasio RB, Metabolism of pyrimidine analogues and their nucleosides. *Pharmacol Ther* **14**: 189–222, 1990.
4. Koenig H and Patel A, Biochemical basis for fluorouracil neurotoxicity. The role of Krebs cycle inhibition by fluoroacetate. *Arch Neurol* **23**: 155–160, 1970.
5. Pinedo HM and Peters GF, Fluorouracil: Biochemistry and pharmacology. *J Clin Oncol* **6**: 1653–1664, 1988.
6. Matsubara I, Kamiya J and Imai S, Cardiotoxic effects of 5-fluorouracil in the guinea pig. *Jpn J Pharmacol* **30**: 871–879, 1980.
7. Okada R, Karakama T, Kimura S, Toizumi S, Mitsushima T and Yokoyama Y, Neuropathologic study on chronic neurotoxicity of 5-fluorouracil and its masked compounds in dogs. *Acta Neuropathol (Berl)* **63**: 334–343, 1984.
8. Okada R, Shibutani M, Matsuo T and Kuroiwa T, Subacute neurotoxicity of 5-fluorouracil and its derivative, carmofur, in cats. *Acta Pathol Jpn* **38**: 1255–1266, 1988.
9. Okada R, Shibutani M, Matsuo T, Kuroiwa T and Tajima T, Experimental neurotoxicity of 5-fluorouracil and its derivatives is due to poisoning the monofluorinated organic metabolites, monofluoroacetic acid and α-fluoro-β-alanine. *Acta Neuropathol (Berl)* **81**: 66–73, 1990.
10. Sweeny DJ, Barnes S and Diasio RB, Production of cholestasis by 2-fluoro-β-alanine-chenodeoxycholic acid: Possible role of this metabolite in the cholestasis associated with hepatic arterial infusion of fluoropyrimidine. *Proc Am Assoc Cancer Res* **29**: 486, 1988.
11. Sweeny DJ, Barnes S, Heggie GD and Diasio RB, Metabolism of 5-fluorouracil to an *N*-cholyl-2-fluoro-β-alanine conjugate: Previously unrecognized role for bile acids in drug conjugation. *Proc Natl Acad Sci USA* **84**: 5439–5443, 1987.
12. Sweeny DJ, Barnes S and Diasio RB, Formation of conjugates of 2-fluoro-β-alanine and bile acids during the metabolism of 5-fluorouracil and 5-fluoro-2-deoxyuridine in the isolated perfused rat liver. *Cancer Res* **48**: 2010–2014, 1988.
13. Sweeny DJ, Martin M and Diasio RB, *N*-Chenodeoxycholyl-2-fluoro-β-alanine: A biliary metabolite of 5-fluorouracil in humans. *Drug Metab Dispos* **16**: 892–894, 1988.
14. Sweeny DJ, Daher G, Barnes S and Diasio RB, Biological properties of the 2-fluoro-β-alanine conjugates of cholic acid and chenodeoxycholic acid in the isolated perfused rat liver. *Biochim Biophys Acta* **1054**: 21–25, 1990.
15. Johnson MR, Barnes S, Sweeny DJ and Diasio RB, 2-Fluoro-β-alanine, a previously unrecognized substrate for bile acid coenzyme A : amino acid : *N*-acyltransferase from human liver. *Biochem Pharmacol* **40**: 1241–1246, 1990.
16. Malet-Martino MC, Bernadou J, Martino R and Armand JP, ^{19}F NMR spectrometry evidence for bile acid conjugates of α-fluoro-β-alanine as the main biliary metabolites of antineoplastic fluoropyrimidines in humans. *Drug Metab Dispos* **16**: 78–84, 1987.
17. Hull WE, Port RE, Herrmann R, Britsch B and Kunz W, Metabolites of 5-fluorouracil in plasma and urine, as monitored by ^{19}F nuclear magnetic resonance spectroscopy, for patients receiving chemotherapy with or without methotrexate pretreatment. *Cancer Res* **48**: 1680–1688, 1988.
18. Zhang R, Barnes S and Diasio RB, Disposition and metabolism of 2-fluoro-β-alanine conjugates of bile acids following secretion into bile. *Biochim Biophys Acta* **1096**: 179–186, 1991.
19. Heggie GD, Sommadossi JP, Cross DS, Hunter WJ and Diasio RB, Clinical pharmacokinetics of 5-fluorouracil and its metabolites in plasma, urine, and bile. *Cancer Res* **47**: 2203–2206, 1987.
20. Coustere C, Mentre F, Sommadossi JP, Diasio RB and Steimer JL, A mathematical model of the kinetics of

5-fluorouracil and its metabolites in cancer patients. *Cancer Chemother Pharmacol* **28**: 123–129, 1991.
21. Zhang R, Soong S-j, Liu T, Barnes S and Diasio RB, Pharmacokinetics and tissue distribution of 2-fluoro-β-alanine in rats. Potential relevance to toxicity pattern of 5-fluorouracil *Drug Metab Dispos* **20**: 113–119, 1992.
22. Bates DM and Watts DG, *Nonlinear Regression Analysis and Its Applications*. John Wiley, New York, 1988.
23. Seber GAF and Wild CJ, *Nonlinear Regression*. John Wiley, New York, 1989.
24. Metzler CM, Estimation of pharmacokinetic parameters; Statistical considerations. *Pharmacol Ther* **13**: 543–556, 1981.
25. D'Argenio DZ and Schumitzky A, *ADAPT II User's Guide. Biomedical Simulations Resource*. University of Southern California, Los Angeles, 1990.
26. Landaw EM and DiStefano JJ, Multiexponential, multicompartmental, and noncompartmental modeling. II. Data analysis and statistical considerations. *Am J Physiol* **246**: R665–R677, 1984.
27. Griffith OW, β-Amino acids: Mammalian metabolism and utility as α-amino acid analogues. *Annu Rev Biochem* **55**: 855–878, 1986.
28. Wright CE, Tallan HH and Lin YY, Taurine: Biological uptake. *Annu Rev Biochem* **55**: 427–453, 1986.